The Gauss-Newton Method in the Problems of Optimizing the Phase Function Calculation Based on the Hilbert Diagnostic Data

Eduard Arbuzov [1,2], Vitaly Arbuzov [1], Yuri Dubnishchev [1] and Olga Zolotukhina [1]

[1] *Kutateladze Institute of Thermophysics SB RAS, Novosibirsk, 630090, Russia*
[2] *Sobolev Institute of Mathematics SB RAS, Novosibirsk, 630090, Russia*

Abstract

The problem of reconstructing the phase function in the Hilbert diagnostics of gaseous, condensed and reacting media is discussed in the paper. The method for restoring the phase disturbances structure of a probing light field based on the iterative Gauss-Newton algorithm is proposed. It does not require the definition of second derivatives and significantly reduces the number of computes. The method consists in successive selection of the phase profile given by the Bezier curve and calculation of the hilbertogram. The reliability of the results is the coincidence of the reference and reconstructed hilbertograms local extrema. The Jacobian matrix of the nonlinear integral operator of the Hilbert visualization is calculated. The proposed algorithm has been certified on test functions. The development of the method and its applications is associated with the processing of experimental results, including complex structures, where the phase function is represented by several Bezier polynomials.

Keywords

Hilbert optics, phase function, optimization, Gauss-Newton method.

1. Introduction

The Hilbert diagnostics of phase structures is the most important result of the methods fruitful synthesis developed in optics and radio engineering [1, 2]. This is an integral operation that signal energy redistributes in a given band of spatial frequencies of the probing field perturbed by the medium under study. The energy loss of the optical signal is minimized in this case. The Hilbert transform in the frequency space is reduced to a certain type of phase transformation of the signal Fourier spectrum with energy conservation in a wide frequency band.

The Hilbert diagnostics results of reacting jets and flames were presented earlier in [3, 4]. The method based on polychromatic Hilbert visualization of phase optical density fields with temperature profile measurements in selected sections of the medium under study is described using the example of studying an axisymmetric hydrogen-air diffusion flame and a candle flame. The phase structure of the probing light field, perturbed by the medium under study, is described in the axial symmetry approximation of the flame using the Abel transform. An iterative selection of radial temperature profiles adapted by Bezier curves, followed by the spatial structure calculation of the refractive index and the phase function, is performed. The criterion for the results reliability of the study is the comparison of the hilbertograms obtained in the experiment with the hilbertograms reconstructed in the approximation of the flame axial symmetry.

The Gauss-Newton method application [5, 6] is proposed to iterative algorithm optimize for reconstructing the phase function in Hilbert diagnostics in this paper. This is an iterative numerical method for solving the least squares problem, a Newton's method modification for finding the objective function minimum. It does not require the second derivatives definition, unlike Newton's method, which

greatly simplifies and reduces the calculations number [7]. Various modifications of the Gauss-Newton method that increase the convergence rate and reduce of the ill-posedness influence in the formulation problem (in particular, the Levenberg-Marquardt algorithm [11]) are presented in [8-10]. The Gauss-Newton method is effective in solving many optimization problems, it is easy to implement and is present in most software packages for applied mathematics.

2. Inverse problem of phase function reconstructing from hilbertramms

Let us turn to figure 1, where the selected section $\hat{y}$ of the studied phase object with a radial distribution of the refractive index n(r) is shown in a simplified way, the z axis coincides with the direction of the probing light beam.
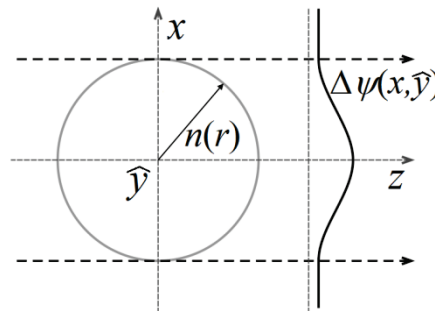

Figure 1: Scheme for diagnosing a phase object (axisymmetric approximation): $n(r)$ – radial distribution of the refractive index

Phase perturbations $\Delta\psi(x, \hat{y})$ of the probing light field that has passed through the medium under study depend on the geometric path length and the refractive index $n(x, \hat{y}, z)$:

$$\Delta\psi(x, \hat{y}) = \frac{2\pi}{\lambda} \int_{z_1}^{z_2} [n(x, \hat{y}, z) - n_\infty]dz,$$

where λ is the wavelength, n_∞ is the refractive index of air, z_1 and z_2 are the entry and exit points of the beam from the object.

The nonlinear integral operator of the first kind is a mathematical model of the Hilbert visualization of the phase shift $\Delta\psi(x, \hat{y})$:

$$H[\Delta\psi](x^*, \hat{y}) = \left\{ \int_{-\infty}^{+\infty} \frac{\cos[\Delta\psi(x, \hat{y})]}{x^* - x} dx \right\}^2 + \left\{ \int_{-\infty}^{+\infty} \frac{\sin[\Delta\psi(x, \hat{y})]}{x^* - x} dx \right\}^2. \tag{1}$$

The inverse problem consists in reconstructing the function $\Delta\psi(x, \hat{y})$ from the $H[\Delta\psi](x^*, \hat{y})$ values, which are recorded in the experiment.

The method based on the successive selection of the profile $\Delta\psi(x, \hat{y})$ and calculation of the hilbertogram $H[\Delta\psi](x^*, \hat{y})$ is proposed for the solution. The local extrema coincidence of the experimental and reconstructed hilbertograms serves as a criterion for stopping the procedure.

The desired phase perturbation function $\Delta\psi(x, \hat{y})$ in the section $\hat{y}$ on the interval $[-r_0, r_0]$ is modeled by Bernstein polynomials of the *n*-th order (Bezier curves) in the smooth fields case [12]:

$$\Delta\psi(x, \hat{y}) = \begin{cases} x(t, P_x) = \sum_{m=0}^{n} P_{x,m}\, b_{m,n}(t) \\ y(t, P_y) = \sum_{m=0}^{n} P_{y,m}\, b_{m,n}(t) \end{cases}; \qquad t \in [0,1]; \tag{2}$$

where $(P_{x,m}, P_{y,m})$ are the vectors components of the reference vertexes, $b_{m,n}(t)$ are the basis functions of the Bezier curve, called Bernstein polynomials:

$$b_{m,n}(t) = \frac{n!}{m!\,(n-m)!}\, t^m (1-t)^{n-m},$$

n is the polynomial degree, m is the ordinal number of the reference vertex. The function $\Delta\psi(x,\hat{y}) = 0$ outside the interval $[-r_0, r_0]$.

The equality $\Delta\psi[x(t),\hat{y}] = y(x(t))$ is valid in the section $\hat{y}$ for the phase function (2) and any parameter t, while $\Delta\psi(x,\hat{y})$ depends on the coordinates of the reference points $\vec{P}$. Denote its Hilbert image by $H_{\vec{P}}^{opt}$. It is calculated taking into account formula (1) as follows:

$$H_{\vec{P}}^{opt}[y](x^*) = \left\{ \int_{-r_0}^{r_0} \frac{\cos[y(x)]}{x^* - x}\,dx \right\}^2 + \left\{ \int_{-r_0}^{r_0} \frac{\sin[y(x)]}{x^* - x}\,dx \right\}^2. \tag{3}$$

As $dx = x_t'(t, P_x)dt$, where $x_t' = dx/dt$, equation (3) can be represented as

$$H_{\vec{P}}^{opt}[y](x^*) = \left\{ \int_0^1 \frac{\cos[y(t,P_y)]}{x^* - x(t,P_x)}\, x_t'(t,P_x)dt \right\}^2 + \left\{ \int_0^1 \frac{\sin[y(t,P_y)]}{x^* - x(t,P_x)}\, x_t'(t,P_x)dt \right\}^2. \tag{4}$$

The optimization problem is to determine those values of the parameters $(P_{x,0}, \dots, P_{x,n})$ and $(P_{y,0}, \dots, P_{y,n})$, at which the objective function minimum is reached:

$$f(\vec{P}) = \left\| F(\vec{P}) \right\|^2 = \sum_{k=0}^{N} \left[H^{ref}(x_k) - H_{\vec{P}}^{opt}(x_k) \right]^2, \quad x_k \in [-r_0, r_0], \tag{5}$$

where H^{ref} is the hilbertogram recorded in the experiment (reference data).

2.1. Gauss-Newton method

In general terms, the optimization problem is to find the extremum (minimum) of the objective function:

$$f(\vec{u}) = \|F(\vec{u})\|^2 = \sum_{k=0}^{N} [a_k(\vec{u}) - b_k]^2,$$

$$\vec{u} = (u_1, \dots, u_m) \in \mathbb{R}^m.$$

The iterative Gauss-Newton method, which uses the Jacobian matrix J of first-order derivatives of the function $F(\vec{u})$ to find the vector $\vec{u_*}$ that minimizes $f(\vec{u})$, is one way to solve this problem.

The Jacobian matrix is determined by the formula [13, 14]:

$$J(\vec{u}) = \left[\frac{\partial a_k(\vec{u})}{\partial u_j} \right]_{k=1, j=1}^{N,m}.$$

The Gauss-Newton method consists in performing successive approximations $\overrightarrow{u_{q+1}}$ according to the expression:

$$\overrightarrow{u_{d+1}} = \overrightarrow{u_d} - \alpha[J^T(\overrightarrow{u_d})J(\overrightarrow{u_d})]^{-1}J^T(\overrightarrow{u_d})F(\overrightarrow{u_d}), \tag{6}$$

where d is the iteration number, α is the coefficient used to regulate the optimization "step" [6], J^T is the transposed matrix.

Denote

$$H_k^{ref} = H^{ref}(x_k), \quad H_k^{opt}[y(x(t,P_x), P_y)] = H_{\vec{P}}^{opt}(x_k).$$

Then the objective function components (5) in the case of hilbertogram processing can be written as

$$F = \begin{Bmatrix} H_0^{ref} - H_0^{opt}[y(x(t,P_x), P_y)] \\ \vdots \\ H_N^{ref} - H_N^{opt}[y(x(t,P_x), P_y)] \end{Bmatrix}. \tag{7}$$

The partial derivatives values with respect to the components of the vector $\vec{P}$ of the function (4) will be found to determine the Jacobi matrix J. First, we write down the values of derivatives with respect to P_x coordinates:

$$\frac{\partial H^{opt}}{\partial P_x}(x^*) = \left|\left\{\int_0^1 \frac{\cos[y(t,P_y)]}{x^* - x(t,P_x)} x'_t(t,P_x)dt\right\}^2\right|'_{P_x} + \left|\left\{\int_0^1 \frac{\sin[y(t,P_y)]}{x^* - x(t,P_x)} x'_t(t,P_x)dt\right\}^2\right|'_{P_x} =$$

$$= A_x + B_x.$$

Then

$$A_x = 2\int_0^1 \frac{\cos[y(t,P_y)]}{x^* - x(t,P_x)} x'_t(t,P_x)dt \cdot \left|\int_0^1 \frac{\cos[y(t,P_y)]}{x^* - x(t,P_x)} x'_t(t,P_x)dt\right|'_{P_x}.$$

Since

$$\left|\frac{\cos[y(t,P_y)]}{x^* - x(t,P_x)} x'_t(t,P_x)dt\right|'_{P_x} = \cos[y(t,P_y)] \left|\frac{x'_t(t,P_x)}{x^* - x(t,P_x)}\right|'_{P_x},$$

and

$$\left|\frac{x'_t(t,P_x)}{x^* - x(t,P_x)}\right|'_{P_x} = \frac{|x'_t(t,P_x)|'_{P_x} \cdot [x^* - x(t,P_x)] - x'_t(t,P_x) \cdot |x^* - x(t,P_x)|'_{P_x}}{[x^* - x(t,P_x)]^2},$$

it follows that

$$\left|\frac{\cos[y(t,P_y)]}{x^* - x(t,P_x)} x'_t(t,P_x)dt\right|'_{P_x} = \cos[y(t,P_y)] \frac{w_1 \cdot [x^* - x(t,P_x)] + w_2 \cdot x'_t(t,P_x)}{[x^* - x(t,P_x)]^2},$$

where

$$w_1 = |x'_t(t,P_x)|'_{P_x},$$

$$w_2 = -|x^* - x(t,P_x)|'_{P_x} = |x(t,P_x)|'_{P_x}.$$

Thus

$$A_x = 2\int_0^1 \frac{\cos[y(t,P_y)]}{x^* - x(t,P_x)} x'_t(t,P_x)dt \cdot$$

$$\cdot \left\{\int_0^1 \frac{\cos[y(t,P_y)]}{x^* - x(t,P_x)} w_1 dt + \int_0^1 \frac{\cos[y(t,P_y)]}{[x^* - x(t,P_x)]^2} w_2 \cdot x'_t(t,P_x)dt\right\},$$

or

$$A_x = \{I_1 + I_2\} \cdot 2\int_{-r_0}^{r_0} \frac{\cos[y(x)]}{x^* - x} dx,$$

where

$$I_1 = \int_{-r_0}^{r_0} \frac{\cos[y(x)]}{x^* - x} \cdot \frac{w_1}{x'_t(t,P_x)} dx,$$

$$I_2 = \int_{-r_0}^{r_0} \frac{\cos[y(x)]}{[x^* - x]^2} \cdot w_2 dx. \tag{8}$$

We transform (8) by integration by parts:

$$I_2 = -\int_{-r_0}^{r_0} \frac{|\cos[y(x)] \cdot w_2|'_x}{x^* - x} dx.$$

Since

$$|\cos[y(x)] \cdot w_2|'_x = |\cos[y(x)]|'_x \cdot w_2 + \cos[y(x)] \cdot |w_2|'_x,$$

$$|\cos[y(x)]|'_x = -\sin[y(x)] \frac{y'_t(t,P_y)}{x'_t(t,P_x)},$$

$$|w_2|'_x = \frac{|w_2|'_t}{x'_t(t, P_x)} = \frac{w_1}{x'_t(t, P_x)},$$

then

$$I_2 = \int_{-r_0}^{r_0} \frac{\sin[y(x)]}{x^* - x} \cdot \frac{y'_t(t, P_y)}{x'_t(t, P_x)} \cdot w_2 dx - \int_{-r_0}^{r_0} \frac{\cos[y(x)]}{x^* - x} \cdot \frac{w_1}{x'_t(t, P_x)} dx.$$

As a result, we arrive at the equality

$$A_x = 2 \int_{-r_0}^{r_0} \frac{\cos[y(x)]}{x^* - x} dx \left\{ \int_{-r_0}^{r_0} \frac{\cos[y(x)]}{x^* - x} \cdot \frac{w_1}{x'_t(t, P_x)} dx + \int_{-r_0}^{r_0} \frac{\sin[y(x)]}{x^* - x} \cdot \frac{y'_t(t, P_y)}{x'_t(t, P_x)} \cdot w_2 dx - \right.$$

$$\left. - \int_{-r_0}^{r_0} \frac{\cos[y(x)]}{x^* - x} \cdot \frac{w_1}{x'_t(t, P_x)} dx \right\} =$$

$$= 2 \int_{-r_0}^{r_0} \frac{\cos[y(x)]}{x^* - x} dx \int_{-r_0}^{r_0} \frac{\sin[y(x)]}{x^* - x} \cdot \frac{y'_t(t, P_y)}{x'_t(t, P_x)} \cdot w_2 dx.$$

Similarly, one can show that

$$B_x = -2 \int_{-r_0}^{r_0} \frac{\sin[y(x)]}{x^* - x} dx \int_{-r_0}^{r_0} \frac{\cos[y(x)]}{x^* - x} \cdot \frac{y'_t(t, P_y)}{x'_t(t, P_x)} \cdot w_2 dx.$$

Now we write down the values of derivatives with respect to P_y coordinates:

$$\frac{\partial H^{opt}}{\partial P_y}(x^*) = \left| \left\{ \int_0^1 \frac{\cos[y(t, P_y)]}{x^* - x(t, P_x)} x'_t(t, P_x) dt \right\}^2 \right|'_{P_y} + \left| \left\{ \int_0^1 \frac{\sin[y(t, P_y)]}{x^* - x(t, P_x)} x'_t(t, P_x) dt \right\}^2 \right|'_{P_y} =$$

$$= A_y + B_y.$$

Then

$$A_y = 2 \int_0^1 \frac{\cos[y(t, P_y)]}{x^* - x(t, P_x)} x'_t(t, P_x) dt \left| \int_0^1 \frac{\cos[y(t, P_y)]}{x^* - x(t, P_x)} x'_t(t, P_x) dt \right|'_{P_y}.$$

Since

$$\left| \frac{\cos[y(t, P_y)]}{x^* - x(t, P_x)} x'_t(t, P_x) \right|'_{P_y} = \frac{x'_t(t, P_x)}{x^* - x(t, P_x)} \cdot |\cos[y(t, P_y)]|'_{P_y},$$

$$|\cos[y(t, P_y)]|'_{P_y} = -\sin[y(t, P_y)] \cdot w_2,$$

we get

$$A_y = -2 \int_0^1 \frac{\cos[y(t, P_y)]}{x^* - x(t, P_x)} x'_t(t, P_x) dt \int_0^1 \frac{\sin[y(t, P_y)]}{x^* - x(t, P_x)} x'_t(t, P_x) \cdot w_2 dt,$$

or

$$A_y = -2 \int_{-r_0}^{r_0} \frac{\cos[y(x)]}{x^* - x} dx \int_{-r_0}^{r_0} \frac{\sin[y(x)]}{x^* - x} \cdot w_2 dx.$$

Similarly

$$B_y = 2 \int_{-r_0}^{r_0} \frac{\sin[y(x)]}{x^* - x} dx \int_{-r_0}^{r_0} \frac{\cos[y(x)]}{x^* - x} \cdot w_2 dx.$$

As a result, the Jacobian matrix will have the following form:

$$J = \begin{Bmatrix} \dfrac{\partial H_0^{opt}}{\partial P_{x,0}} & \cdots & \dfrac{\partial H_0^{opt}}{\partial P_{x,n}} & \dfrac{\partial H_0^{opt}}{\partial P_{y,0}} & \cdots & \dfrac{\partial H_0^{opt}}{\partial P_{y,n}} \\ \vdots & \ddots & \vdots & \vdots & \ddots & \vdots \\ \dfrac{\partial H_N^{opt}}{\partial P_{x,0}} & \cdots & \dfrac{\partial H_N^{opt}}{\partial P_{x,n}} & \dfrac{\partial H_N^{opt}}{\partial P_{y,0}} & \cdots & \dfrac{\partial H_N^{opt}}{\partial P_{y,n}} \end{Bmatrix}. \tag{9}$$

The Gauss-Newton algorithm (6), taking into account (7) and (9), will be defined as

$$\overrightarrow{P_{d+1}} = \overrightarrow{P_d} - \alpha[J^T J]^{-1} J^T F(\overrightarrow{P_d}). \tag{10}$$

Thus, optimization begins with setting the vector components $\overrightarrow{P_0}$, which determine the phase function initial profile, then applying formula (10) step by step, and terminating the calculation process when the squared distances sum between the extrema coordinates of the reference and optimized hilbertograms becomes less than the specified value.

3. Algorithm application on the test function example

It is sufficient to determine the phase function only on the interval $[0, r_0]$ in the case of axisymmetric objects.

Let's simulate an example when an axisymmetric object with a section radius $r_0 = 30$ mm is diagnosed. Define $\Delta\psi(x, \hat{y})$ within $0 \le x \le r_0$ as a parametric Bezier curve of the third degree:

$$\Delta\psi(x, \hat{y}) = \begin{cases} x(t) = (1-t)^3 P_{x,0} + 3(1-t)^2 t P_{x,1} + 3(1-t)t^2 P_{x,2} + t^3 P_{x,3} \\ y(t) = (1-t)^3 P_{y,0} + 3(1-t)^2 t P_{y,1} + 3(1-t)t^2 P_{y,2} + t^3 P_{y,3} \end{cases},$$

for $x \ge r_0$ the value $\Delta\psi(x, \hat{y}) = 0$, and we continue it in an even way to the region $-r_0 \le x \le 0$.

The pixel size in the image corresponded to 1/30 mm when registering the optical signal in the experiments [3, 4]. Therefore, the number of samples $N = 1801$ in the interval $[-r_0, r_0]$.

The function graph $\Delta\psi(x, \hat{y})$ and its hilbertogram is shown in figure 2 for the reference points values

$$\{P_{x,0} = 0, P_{y,0} = 50\}, \quad \{P_{x,1} = 15, P_{y,1} = 50\}, \quad \{P_{x,2} = 15, P_{y,2} = 0\}, \quad \{P_{x,3} = 30, P_{y,3} = 0\}.$$
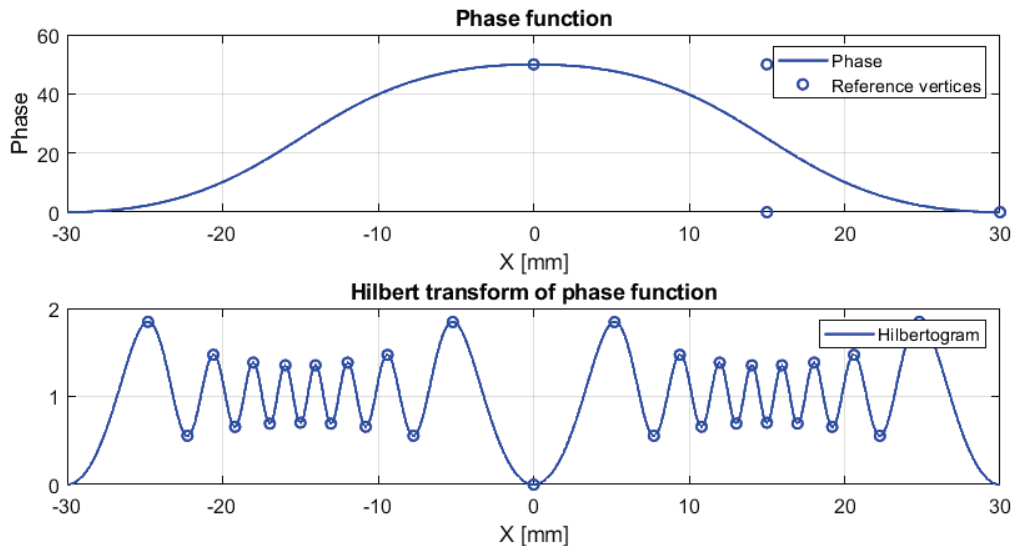

Figure 2: The phase function represented by the Bezier curve (with reference vertices) and the hilbertogram calculated from it. The hilbertogram is presented in a dimensionless form with indication of the local extrema points

The hilbertogram shown in figure 2 will be taken as the reference H^{ref}, and the phase function corresponding to it will be denoted by $\Delta\psi^{ref}$. Let us consider the biased function $\Delta\psi^{opt}$ as an initial approximation, which must be optimized to $\Delta\psi^{ref}$ (figure 3).
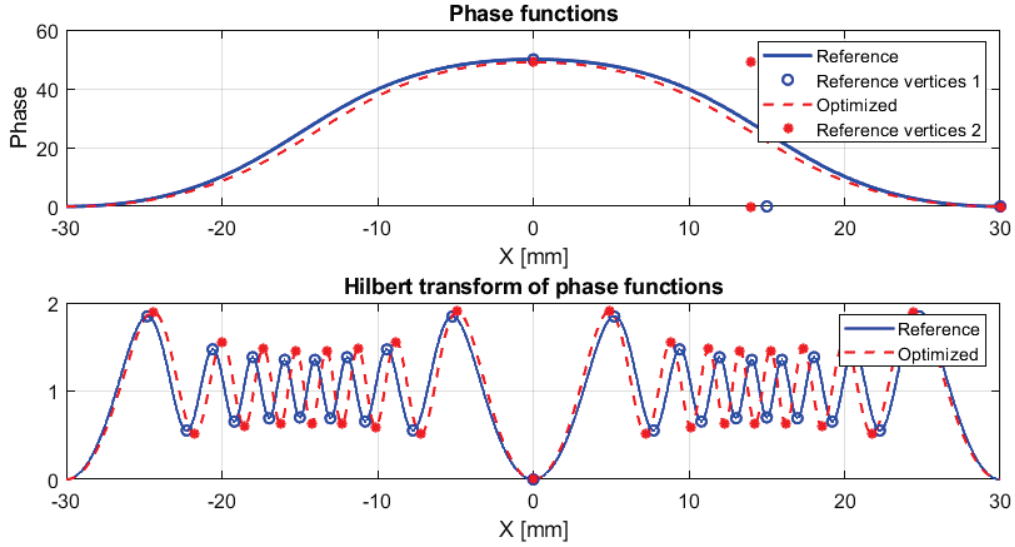
Figure 3: Reference hilbertogram H^{ref} and initial (optimized) hilbertogram H^{opt}, and their corresponding phase functions

In this case, the parameter w_2 for derivatives with respect to the vector $\vec{P}$ will have the values presented in table 1.

Table 1 – Derivatives with respect to $\boldsymbol{P_x}$ and $\boldsymbol{P_y}$ coordinates

Coordinates $\boldsymbol{P_x}$	Coordinates $\boldsymbol{P_y}$	$\boldsymbol{w_2}$
$P_{x,0}$	$P_{y,0}$	$(1-t)^3$
$P_{x,1}$	$P_{y,1}$	$3(1-t)^2 t$
$P_{x,2}$	$P_{y,2}$	$3(1-t)t^2$
$P_{x,3}$	$P_{y,3}$	t^3

The Jacobian matrix will have the following form:

$$J = \left\{ \begin{matrix} \dfrac{\partial H_0^{opt}}{\partial P_{x,0}} & \dfrac{\partial H_0^{opt}}{\partial P_{x,1}} & \dfrac{\partial H_0^{opt}}{\partial P_{x,2}} & \dfrac{\partial H_0^{opt}}{\partial P_{x,3}} & \dfrac{\partial H_0^{opt}}{\partial P_{y,0}} & \dfrac{\partial H_0^{opt}}{\partial P_{y,1}} & \dfrac{\partial H_0^{opt}}{\partial P_{y,2}} & \dfrac{\partial H_0^{opt}}{\partial P_{y,3}} \\ \vdots & \vdots & \vdots & \vdots & \vdots & \vdots & \vdots & \vdots \\ \dfrac{\partial H_N^{opt}}{\partial P_{x,0}} & \dfrac{\partial H_N^{opt}}{\partial P_{x,1}} & \dfrac{\partial H_N^{opt}}{\partial P_{x,2}} & \dfrac{\partial H_N^{opt}}{\partial P_{x,3}} & \dfrac{\partial H_N^{opt}}{\partial P_{y,0}} & \dfrac{\partial H_N^{opt}}{\partial P_{y,1}} & \dfrac{\partial H_N^{opt}}{\partial P_{y,2}} & \dfrac{\partial H_N^{opt}}{\partial P_{y,3}} \end{matrix} \right\}.$$

The root-mean-square error between the hilbertogram extrema H^{ref} and H^{opt} after 12 iterations as a result of applying the Gauss-Newton method (10) has reached the value

$$\sigma_{\text{ср}} = \sqrt{\sum_{q=1}^{Q} \left(H_q^{opt} - H_q^{ref} \right)^2} = 0,0213,$$

where Q is the peaks number of function extrema, while the maximum deviation was

$$\sigma_{max} = \max_{q=1,\ldots,Q} \left| H_q^{opt} - H_q^{ref} \right| = 0,002.$$

The phase function $\Delta\psi^{opt}$ obtained as a result of optimization is shown in figure 4.
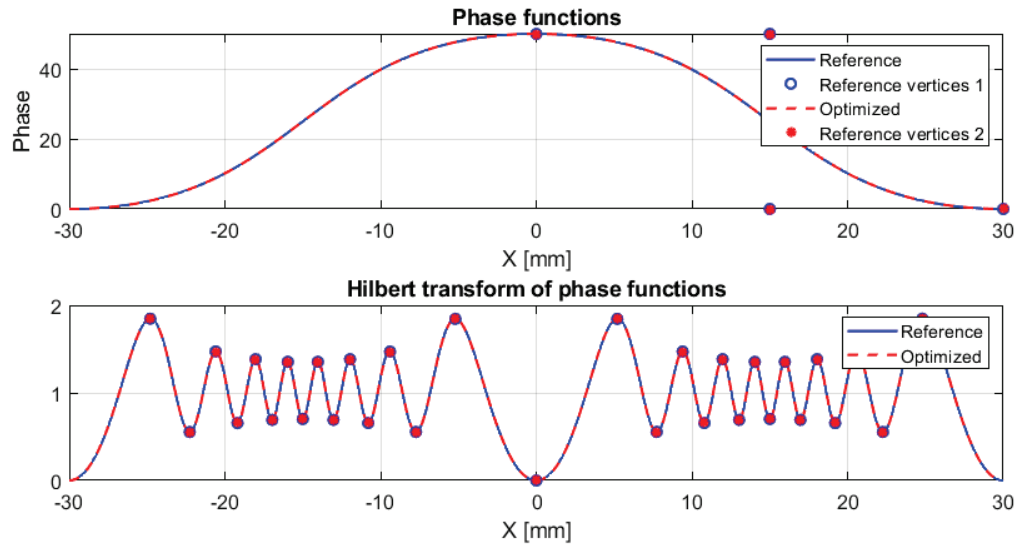
Figure 4: Optimization result

The maximum deviation of $\Delta\psi_{opt}$ from $\Delta\psi_{ref}$ was

$$\sigma_{max}(\Delta\psi) = \max_{k=0,\dots,N}\left|\Delta\psi_k^{opt} - \Delta\psi_k^{ref}\right| = 0{,}0025.$$

4. Conclusion

The Gauss-Newton method, adapted to the problem of determining the phase function from Hilbert diagnostics data of gaseous, condensed and reacting media, is presented in the work. The algorithm for phase structure reconstructing, based on the successive selection of the phase profile given by Bezier polynomial, and the subsequent calculation of the hilbertogram, is given. The criterion for the results reliability is the local extrema coincidence of the reference and reconstructed hilbertograms. The Jacobian matrix calculation for the nonlinear integral operator of Hilbert visualization is done. The operation example of the algorithm for the test function in the case of an axisymmetric problem statement is given.

The algorithm application to the experimental data processing will be the further research direction. The Gauss-Newton method adaptation to the possibility of desired phase function specifying by several Bezier curves in cases of complex structures diagnostics.

5. Acknowledgements

6. References

[1] V. A. Arbuzov, Yu. N. Dubnishchev, Metody gil'bert-optiki v izmeritel'nykh tekhnologiyakh [Hilbert-optics methods in measurement technologies], NSTU University Publ., Novosibirsk, 2007.

[2] L. M. Soroko, Gil'bert-optika [Hilbert optics], Nauka Publ., Moscow, 1981.

[3] V. A. Arbuzov, E. V. Arbuzov, Yu. N. Dubnishchev, V. V. Lukashov, O. S. Zolotukhina, Method of polychromatic Hilbert diagnostics of phase and temperature perturbations of axisymmetric flames, CEUR Workshop Proceedings 3027 (2021) 369–378. doi:10.20948/graphicon-2021-3027-369-378.

[4] V. A. Arbuzov, E. V. Arbuzov, Yu. N. Dubnishchev, V. V. Lukashov, O. S. Zolotukhina, Method of polychromatic Hilbert diagnostics of phase and temperature perturbations of axisymmetric flames, Journal of Physics: Conference Series 2233 (2022). doi:10.1088/1742-6596/2233/1/012006.

[5] C. A. Floudas, P. M. Pardalos, Encyclopedia of optimization, Springer, New York, 2008.

[6] Habr, Levenberg-Marquardt algorithm for non-linear least squares method and its implementation in Python, 2016. URL: http: //habr.com/ru/articles/308626/.

[7] K. P. Lovetsky, L. A. Sevastyanov, O. N. Bikeev, M. V. Paukshto, Matematicheskiy sintez opticheskikh nanostruktur [Mathematical synthesis of optical nanostructures], RUDN University Publ., Moscow, 2008.

[8] N. E. Yudin, Modified Gauss–Newton method for solving a smooth system of nonlinear equations, Computer research and modeling 13 (2021) 697–723. doi:10.20537/2076-7633-2021-13-4-697-723.

[9] M. H. Loke, T. Dahlin, A comparison of the Gauss-Newton and quasi-Newton methods in resistivity imaging inversion, J. Applied Geophysics 49 (2002) 149–162. doi:10.1016/S0926-9851(01)00106-9.

[10] E. H. Bergou, Y. Diouane, V. Kungurtsev, Convergence and complexity analysis of a Levenberg-Marquardt algorithm for inverse problems, J. Optimization Theory and Applications 185 (2020) 927–944. doi:10.1007/s10957-020-01666-1.

[11] V. V. Vasin, The levenberg-marquardt method for approximation of solutions of irregular operator equations, Automation and remote control 73 (2012) 440–449. doi:10.1134/S0005117912030034.

[12] D. F. Rogers, J. A. Adams, Matematical elements for computer graphics (Second Edition), McGraw-Hill, New York, 1990.

[13] V. A. Zorich, Matematicheskiy analiz [Mathematical analysis], part 1, 6st. ed., ICNMO Publ., Moscow, 2012.

[14] N. S. Bakhvalov, N. P. Zhidkov, G. M. Kobelkov, Chislennyye metody [Numerical methods], Binom Publ., Moscow, 2003.